Research Article | Vol. 27, No. 26 / 23 December 2019 / Optics Express 38670
Optics EXPRESS

Studying the different coupling regimes for a plasmonic particle in a plasmonic trap

JEONGHYEON KIM AND OLIVIER J. F. MARTIN*

Nanophotonics and Metrology Laboratory, Swiss Federal Institute of Technology Lausanne (EPFL), EPFL-STI-NAM, ELG Station 11, CH-1015 Lausanne, Switzerland
*olivier.martin@epfl.ch

Abstract: Plasmonic antennas improve the stiffness and resolution of optical tweezers by producing a strong near-field. When the antenna traps metallic objects, the optically-resonant object affects the near-field trap, and this interaction should be examined to estimate the optical force accurately. We study this effect in detail by evaluating the force using both Maxwell's stress tensor and the dipole approximation. In spite of the strong optical interaction between the particle and the antenna, the results show that the dipole approximation remains accurate for calculating forces on Rayleigh particles. For particles whose sizes exceed the dipole limit, we observe different coupling regimes where the force becomes either attractive or repulsive. The distributions of field amplitudes and polarization charges explain such a behavior.

1. Introduction

Following a series of experiments by Ashkin [1,2], optical tweezers have established themselves as successful tools, particularly in biological studies, where they allow viruses, bacteria, and even DNA molecules to be manipulated directly with light [3–6]. The underlying principle is to use a highly focused laser beam to generate a large gradient of the light intensity, which produces a so-called optical gradient force [7]. With the optical tweezers, we can trap and manipulate small particles, typically in the order of microns, including dielectric and metallic ones [7,8]. However, conventional optical trapping also has a limit in its stiffness and resolution, especially when manipulating nanoscale particles [2,9,10]. Due to the decrease in the viscous drag for small particles, the Brownian motion let tiny particles easily escape from the trap. Furthermore, the optical force also scales down with the volume of the object [9]. Another issue is the diffraction limit of the trapping laser: an object much smaller than the focal spot or the beam waist experiences unstable trapping [2]. As a result, the manipulation of nanoscale particles is inherently challenging [9,10]. In order to enhance the trapping stiffness of such small objects, one can increase the power of the trapping laser for example [2], or implement an alternative trapping geometry such as counter-propagating beams [11].

Near-field optics and plasmonics have provided another possibility to achieve nanoscale manipulation by focusing light below the diffraction limit and locally amplifying the fields [12–20]. Plasmonic antennas are metallic, mostly gold or silver, nanostructures where their conduction electron clouds can resonantly oscillate through optical illumination [21,22]. Under resonant conditions, the electron oscillations produce a strong near-field, which decays very rapidly in space; thus, the enhanced field gradient around the antenna provides additional confinement for trapping, overcoming the diffraction limit [23,24]. Plasmonic antennas also amplify fields through localization, which can also improve the trapping stiffness [25].

Metallic nanoparticles, thanks to their strong optical response, are very good candidates for nanoscale manipulation. A previous belief on metallic particles was that they are difficult to trap due to their highly reflecting properties [26,27]. Another issue was that metallic particles have resonant characteristics like plasmonic antennas, which can significantly alter the trapping conditions on resonance [28]. However, metallic particles are found to experience either an

#379435 https://doi.org/10.1364/OE.379435
Journal © 2019 Received 1 Oct 2019; revised 23 Nov 2019; accepted 7 Dec 2019; published 20 Dec 2019

Optics EXPRESS

attractive or repulsive force depending on the incident wavelength [29–31]. This behavior originates from the wavelength-dependent scattering, absorption, and polarizability of plasmonic particles. In particular, experimental studies have shown that metallic particles can be stably trapped when illuminated with infrared light since they behave like a high refractive index dielectric particle at wavelengths longer than the resonance [32–35]. Since the trapping force is proportional to the polarizability of a particle, it is especially strong for a metallic particle that has large polarizability [36]. This compensates for the decrease in optical force associated with the small volume of nanoscale particles.

A combination of plasmonic antennas and metallic nanoparticles is appealing for the precise positioning of single nanoscale objects. However, special attention must be paid in this case because both the trap, i.e. the antennas, and the trapped metallic objects can be optically excited and can furthermore interact with each other. Although several experiments have demonstrated plasmonic trapping [13–16,18,19,24], the sheer resonant characters of both the trap and the trapped particle call for studies on the coupling between these two resonant structures and the influence of this coupling on the optical forces.

Here, we theoretically study the optical force exerted on a metallic particle trapped by a plasmonic dipole antenna. We investigate the change in optical force as a function of the particle size, position, and incident wavelength (throughout we refer to the particle diameter as its size). A priori, one would think that the influence of the metallic particle on the near-field of the antenna can significantly influence the field distribution and therefore the optical force. In practice, this would imply that only full-field calculations taking into account both the plasmonic dipole antenna and the trapped particle can accurately capture the physics of the system. Quite surprisingly, it appears that the dipole approximation remains accurate, even in such an intricate system, when the particle size is small enough to apply that approximation. We confirm this by comparing the force obtained from full-field calculations that consider the self-consistent system with those from an analytical equation that assumes the particle as a mere induced dipole. In the second half of the paper, we also study the force acting on a wide range of particle sizes (10 – 200 nm) with the full-field calculations. We evidence attractive and repulsive behaviors for particles larger than 150 nm in the presence of a plasmonic antenna.

2. Results and discussion

2.1. Plasmonic dipole antenna

We consider a nanoscale dipole antenna as a plasmonic optical tweezer. The dipole antenna consists of two gold nanorods separated by a gap. Each nanorod is a rounded rectangular cuboid (90 nm length, 40×40 nm^2 cross-section) and the gap is set to be 30 nm. We choose a 30 nm gap size, such that a 20 nm spherical particle, which is the target object to trap here, can pass through the gap. For all the simulations throughout the paper, we put the antenna in a Cartesian coordinate system with the origin at the center of the gap and the longitudinal axis of the antenna along the x-axis. We set the dielectric constant of gold from Johnson and Christy [37] and that for the medium to be 2.013, an average of water (1.77, superstrate) and glass (2.25, substrate), to mimic the effect of a substrate [38,39]. The incident light propagates along the $+z$-direction, polarized along the x-axis (Fig. 1a, inset) with the power intensity of 4 mW/μm^2.

2.2. Full Maxwell's stress tensor and dipole approximation methods for optical forces

When we place a metallic nanoparticle in the near-field around the antenna, the spatially varying near-field induces a force on the particle. Furthermore, since the metal particle is close to the antenna, the particle can modify the near-field due to a strong interaction with the antenna. Depending on the size and the location of the particle, the field disturbance caused by the

Optics EXPRESS

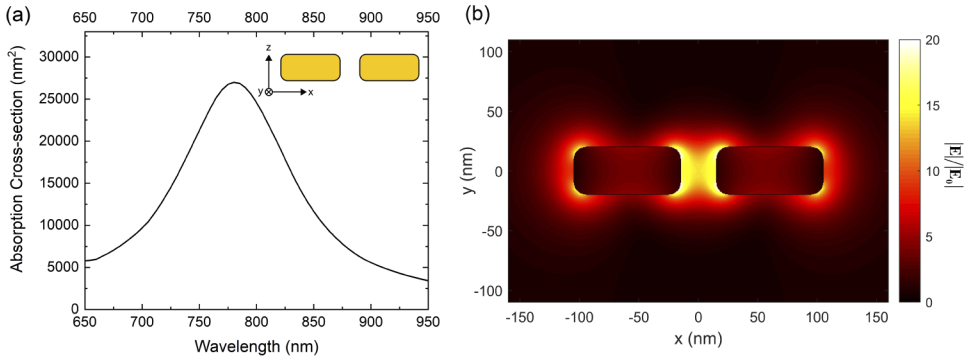

Fig. 1. Gold dipole antenna used in this study. The antenna consists of two nanorods with dimensions $90 \times 40 \times 40$ nm^3 separated by a 30 nm gap. The light is incident in the $+z$-direction, polarized along the x-axis. (a) Absorption cross-section and (b) electric near-field amplitude enhancement factor at $\lambda = 780$ nm; the gradient of this enhanced near-field exerts an optical force on an object located nearby.

interaction may well be significant or negligible. We shall study this effect by computing the optical force using two different approaches.

The first approach is based on Maxwell's stress tensor, with which we compute the time-averaged optical force $\mathbf{F}$ by integrating the stress tensor $\mathbf{T}$ on the surface of the particle S:

$$\langle \mathbf{F} \rangle = \int_S \langle \mathbf{T}(\mathbf{r}, t) \rangle \cdot \mathbf{n}(\mathbf{r}) ds, \tag{1}$$

where the expression $\langle \cdots \rangle$ denotes the time average, $\mathbf{r}$ the position vector, $\mathbf{n}$ the outward unit vector normal to the surface, and ds an infinitesimal surface element. In the remaining of the paper, we refer to this approach as the Maxwell's stress tensor (MST) approach.

The Maxwell's stress tensor $\mathbf{T}$ is commonly expressed as a function of electric ($\mathbf{E}$) and magnetic ($\mathbf{H}$) fields; here we obtain it directly from the surface integral equation (SIE) formulation of Maxwell's equations [40,41]. We use the SIE formulation throughout this paper to simulate the interaction of light with plasmonic structures. The SIE is related to the boundary element method and gives accurate and reliable solutions for plasmonic nanostructures under resonant conditions [40]. For the derivation of SIE and its direct use for the computation of MST, we refer to Refs. [40] and [41]. We also provide open datasets from the SIE formulation and its analysis for calculating the force and other physical values such as field enhancement factors and scattering cross-sections in Ref. [42].

The second approach starts by assuming that the particle is sufficiently smaller than the illumination wavelength (with a particle size < 1/10 the background wavelength) to behave like an induced point dipole. By approximating the particle as a point-like dipole, this method does not take into account the influence of the particle' s physical boundary onto the near-field. We first evaluate the near-field generated by the antenna alone at the location of the particle and then find an analytical solution for a time-averaged force with the electric field at the particle position [43].

We assume an arbitrary monochromatic electromagnetic wave with angular frequency ω, which describes the near-field generated by the antenna. With the assumption of time-harmonic fields with the form $\exp(-i\omega t)$ [36], the induced dipole moment of the particle is proportional to the electric field at the particle position $\mathbf{r_0}$ [44]:

$$\mathbf{p} = \varepsilon_m \alpha(\omega) \mathbf{E}_0(\mathbf{r}_0), \tag{2}$$

Optics EXPRESS

where ε_m is the relative permittivity of the surrounding medium and α is the polarizability of the particle. The polarizability α is the parameter that includes the size information of the particle; under the dipole approximation, it can be expressed as [36]:

$$\alpha(\omega) = 4\pi\varepsilon_0 a^3 \frac{\varepsilon - \varepsilon_m}{\varepsilon + 2\varepsilon_m}, \tag{3}$$

with the parameters ε_0 denoting the permittivity of the free space, ε the relative permittivity of the particle, and a the radius of the particle. The relative permittivities in Eqs. (2) and (3) are those appropriate to the incident frequency ω. The time-averaged force exerted by an arbitrary electromagnetic field can then be evaluated as [43,44]:

$$\langle \mathbf{F} \rangle = \sum_i \frac{1}{2} \mathrm{Re}\{p_i^* \nabla E_{0i}\}, \tag{4}$$

where p_i^* and E_{0i} $(i = x, y, z)$ are respectively the complex conjugates of the dipole moments and the electric field components of a three-dimensional Cartesian coordinate system. Since this approach is based on the dipole approximation, we will refer to it as the dipole approximation (DA) method.

Let us emphasize that while the MST method provides a self-consistent solution that includes the interaction between the trapped particle and the trapping antenna, the DA method does not include this interaction, and the optical force is merely computed from the near-field distribution produced by the antenna in the absence of the particle. Since the interaction between a metallic particle and a plasmonic antenna can be very strong [45], we would anticipate that the MST method provides a much better accurate description of the optical force. The first half of this article aims at clarifying this point.

Using the MST and DA methods, we first compare the optical force vectors when moving a spherical gold nanoparticle with a 20 nm diameter (the green circle in Fig. 2) above the antenna. We assume that a monochromatic plane wave at $\lambda = 800$ nm, close to the resonance of the antenna, comes from the bottom of the figure (in the $+z$-direction). We change the position of the particle between -150 nm and 150 nm in the x-direction while keeping the spacing between the bottom surface of the particle and the top surface of the antenna to 5 nm. The red and black arrows show a line of force vectors calculated using the MST and DA methods, respectively. The values computed with MST (red arrows) are larger than those computed with DA (black arrows), especially where the field is extreme, at each corner of the nanorods. This implies that the interaction between the particle and the antenna becomes stronger when the particle is located at those extreme fields. It also indicates that the interaction between the particle and the antenna works in a way that reinforces the fields and therefore the optical force. This is in agreement with the binding interaction that is evidenced within the hybridization model [29].

The optical force depends on the wavelength of the incoming plane wave due to the resonant characteristics of the antenna. In Fig. 3(a), we compute the vertical component of the optical force (along the z-axis) as a function of the wavelength of incident light while fixing the position of the 20 nm diameter gold nanoparticle 5 nm above the top of the antenna (i.e., the particle center is 35 nm above the center of the gap, viz. the origin). The negative sign of the force means an attraction towards the gap. Both MST and DA methods result in similar wavelength-dependent forces with less than approximately 10 % difference, although the solution from MST always shows larger forces than that from DA for the range of calculations. The MST method also shows the force spectrum slightly red-shifted compared to that of the DA method since it includes the nanoparticle and its hybridization with the antenna, which lowers the energy of the system, leading to a redshift [29,46].

While the two calculation methods show a good agreement in the previous case, they can also give considerably different results, especially when the particle stands between the corners of the

Optics EXPRESS

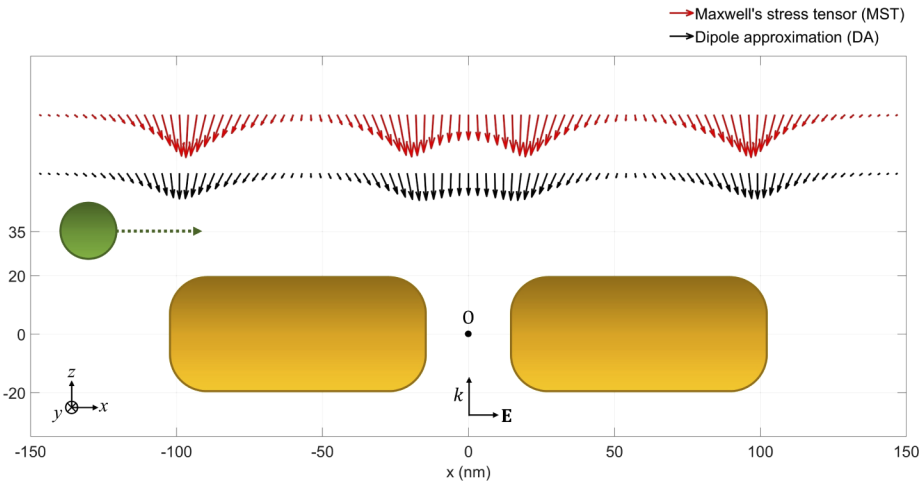

Fig. 2. Optical force vectors for a 20 nm gold nanoparticle (green disk), as a function of its position along the x-axis. The spacing between the bottom surface of the nanoparticle and the top surface of the antenna is 5 nm and the illumination wavelength is $\lambda = 800$ nm. The optical force vector at each position is computed 1) analytically using the dipole approximation (DA, the black arrows) or 2) numerically using the Maxwell's stress tensor (MST, the red arrows); the corresponding data are shifted vertically for legibility.

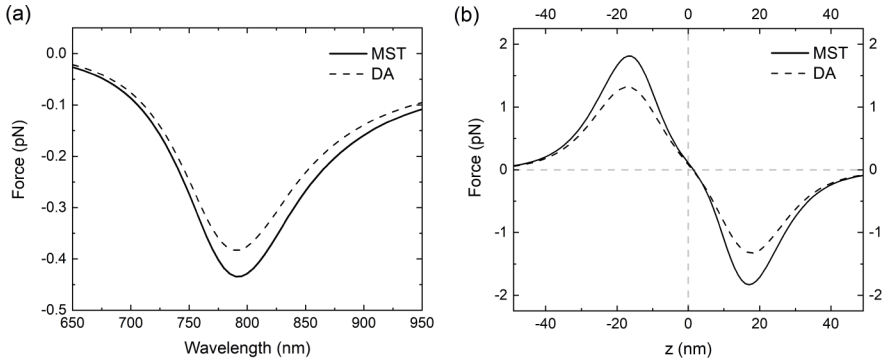

Fig. 3. Comparison between DA and MST calculations for a 20 nm spherical gold nanoparticle. (a) Force as a function of the illumination wavelength when the particle is fixed at (0, 0, 35 nm), which is 5 nm above the antenna top surface. (b) Force when the particle is moved along the z-axis in the center of the gap (x = y = 0) while the incident wavelength is fixed as $\lambda = 800$ nm.

nanorods where it feels the most substantial field gradient. In Fig. 3(b), we evaluate the force as a function of the particle position while the particle passes through the gap of the antenna vertically along the z-axis. The difference in the force becomes prominent when the particle becomes closer to the points where the gradient of the field is most significant, i.e. the force magnitude is the largest. Like in the case of Fig. 3(a), this difference implies the active involvement of the particle in the field since the DA method does not include such influence [17].

This effect stands out more when increasing the size of the particle while fixing its position between the top corners where the field is strongest, i.e. at the point (0, 0, 20 nm). In Fig. 4, we evaluate the magnitude of the trapping force for different particle sizes ranging from 5 to 30 nm (incident wavelength $\lambda = 800$ nm). The force magnitude increases to the third power of the

Optics EXPRESS

diameter when we use the dipole approximation since the polarizability is proportional to the particle volume [44]. When we introduce the actual particle geometry for numerical calculations with MST, the gaps formed between the particle and the corners of the antenna enhance the field, leading to significantly greater forces for larger particles. For instance, the force for the 30 nm-diameter particle, where the additional gap size goes down to 2 nm, becomes 2.8 times larger than that from the DA method.

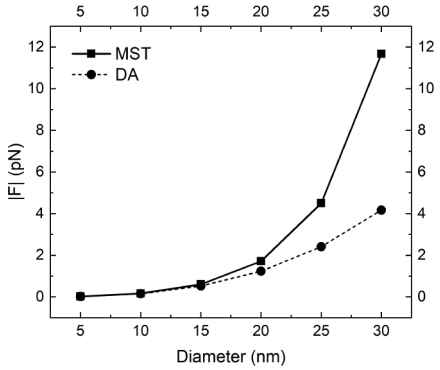

Fig. 4. Optical forces acting on particles with different sizes, centered at the point (0, 0, 20 nm), where the field is strongest (λ = 800 nm).

2.3. *Wavelength and particle size dependence of the optical force*

As seen in Figs. 3 and 4, the force depends on the particle size, the illumination wavelength as well as the location of the particle. Here we look in greater detail into the influences of these parameters on the optical force, whereas the previous section was dedicated to the comparison between the numerical and analytical methods. We use the MST method since it predicts the near-field acting on a particle more accurately by taking into account the field modification caused by the particle, and also because the dipole approximation is not valid anymore for particles exceeding the Rayleigh regime.

In Fig. 5, we plot the optical force as a function of the particle size (10 – 200 nm, the x-axis) and the illumination wavelength (λ = 650 – 950 nm, 5 nm step, the y-axis). In order to vary the particle diameter up to 200 nm without changing gaps and hence varying coupling between the particle and the antenna, we fix the distance between the bottom of the particle and the top surface of the antenna to be 5 nm and move the particle center accordingly, as shown in the inset of Fig. 5.

In this wide range of sizes, interesting features start to appear. First, the force increases with the diameter up to 100 nm, and then it decreases above this size. However, for particle size larger than 160 nm, we discover a different regime whereby the force becomes either attractive or repulsive, depending on the wavelength. To better understand the physics behind these complicated features, we selected four different parameter sets indicated as A, B, C, and D in Fig. 5, which represent different coupling regimes. We first analyze the resonance spectra of the coupled particle-trap system for those instances (Fig. 6) and look into further details by evaluating the near-fields and surface polarization charges (Fig. 7).

In Fig. 6, we show the absorption cross-sections of the system including both the antenna and the particle as the resonance spectra of the coupled particle-trap system. The grey solid lines in each figure represents the response of the antenna only, and they are plotted together to show how the coupling affects the resonance spectrum. The force spectra on the corresponding particles are shown together as dashed lines. The force spectrum is reversed in the vertical axis to make the

Optics EXPRESS

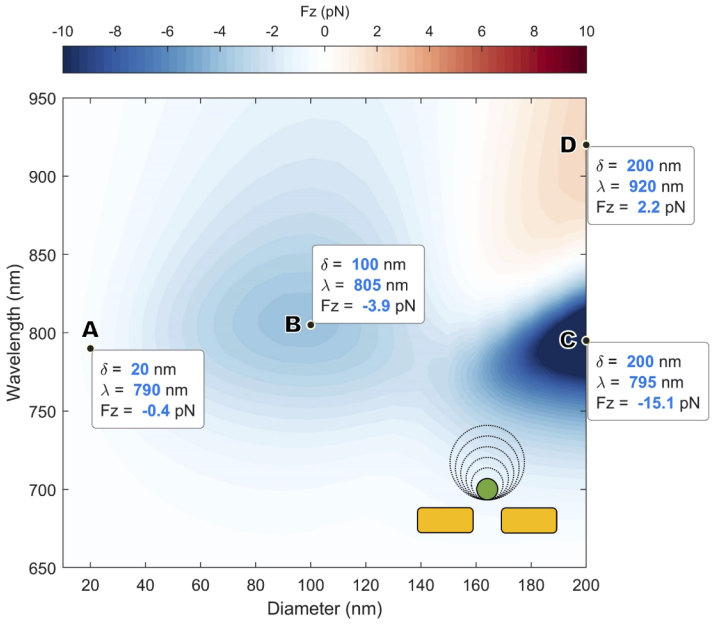

Fig. 5. Size and wavelength dependence of the optical force using the MST approach. The gold nanoparticle diameter δ is varied from 10 nm to 200 nm. The bottom of the nanoparticle is fixed 5 nm above the top surface of the dipole antenna to maintain the physical gap, while its center position is moved accordingly, as sketched in the inset (Bottom right). We analyze the points A, B, C, and D in Fig. 7.

comparison with the resonance spectrum easy. The instances A, B, C, and D from Fig. 5 are also indicated on the force spectra.

Often the active involvement of the particle in optical trapping is described in the context of a self-induced back-action (SIBA) trapping [17]. For metallic particles, the SIBA effect can be even more prominent by changing the resonant response of the system itself. Figure 6 shows that the resonant response of the system is strongly modified by the presence of the trapped particle, especially when the particle size is comparable to that of the trap. The coupled system shows redshifts for all the instances investigated, which implies that the mode of the antenna is hybridized with that of the particle to lower the energy, forming a bonding mode [29]. In particular, depending on the strength of the coupling, the spectrum with the particle can remain similar (Figs. 6(a) and 6(b)) or become very different (Fig. 6(c)) from that of the trap.

Most importantly, Fig. 6 shows that the force spectrum follows the spectrum of the coupled system, rather than that of the sole antenna. This gives evidence on the active involvement of the particle in trapping. For more detailed analysis, we study the distribution of the near-fields and surface polarization charges on the points indicated as A, B, C, and D in Figs. 5 and 6 in the following.

The near-fields and polarization charges on the nanostructure surfaces show how the particle couples with the antenna. In particular, the polarization charges are typically a complex quantity, and we shall report both its real and imaginary parts since they together provide information about the phase shift between the incident light and the charge oscillations as well as the amplitude of the response [47]. For example, depending on the excitation frequency, a time-harmonic forced oscillator is not oscillating in phase with the driving force but lags by a certain amount of phase that becomes 90° on resonance. This 90° phase lag moves all the information to the imaginary part so that we must look at both the real and imaginary parts for accurate analysis.

Optics EXPRESS

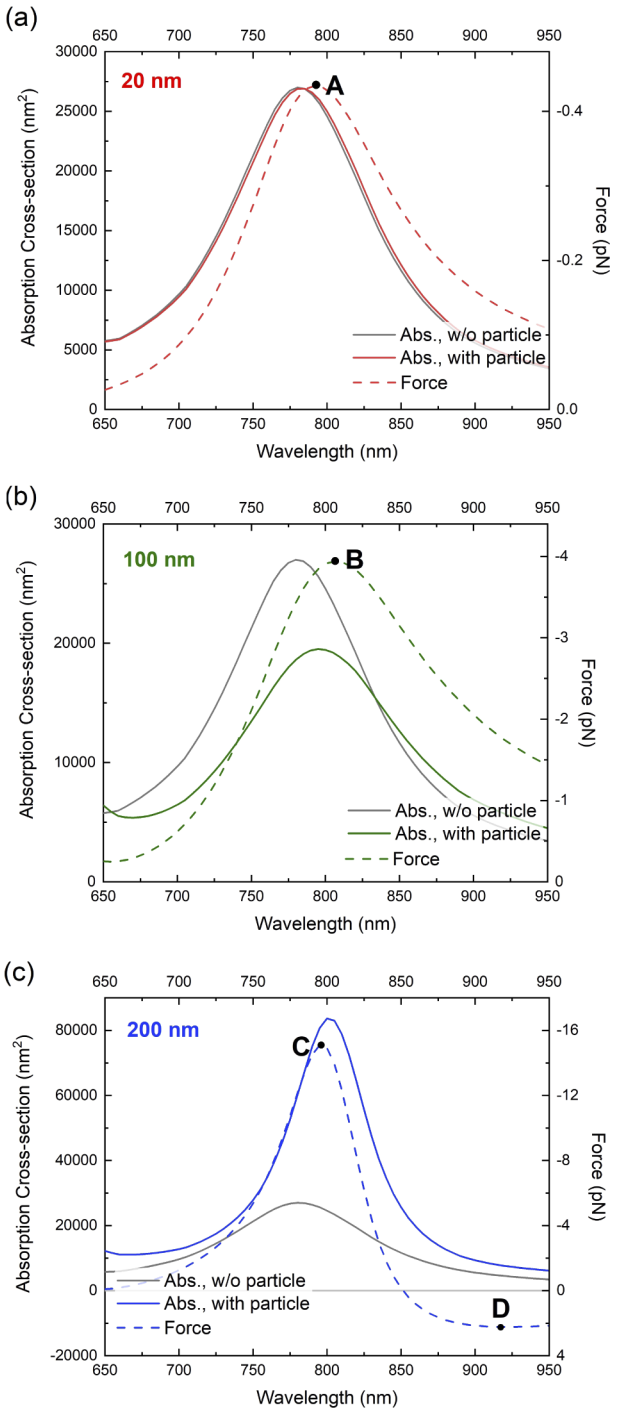

Fig. 6. Resonance spectra of the coupled particle-trap system for the particle size of (a) 20 nm, (b) 100 nm, and (c) 200 nm. The force exerted on the corresponding particle is plotted as dashed lines. The response of the trap itself (without particle) is shown as grey solid lines for comparison. The instances A, B, C, and D from Fig. 5 are indicated on the force spectra.

Optics EXPRESS

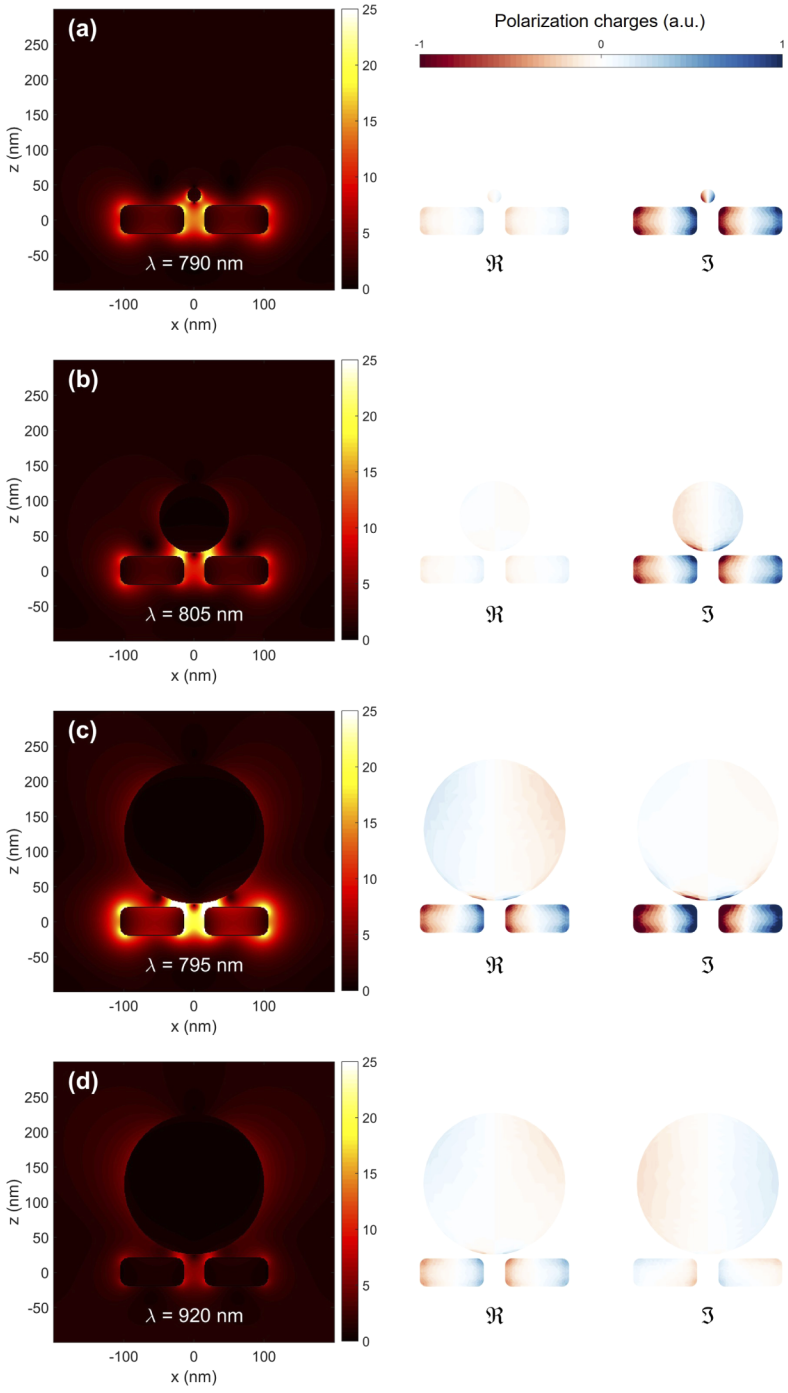

Fig. 7. (*Left*) Near-field amplitude distributions and (*Right*) real $\Re$ and imaginary $\Im$ parts of the polarization charges on the nanostructure surfaces. The parameter sets marked as A, B, C, and D in Fig. 5 are analyzed to represent different coupling regimes. (a) Nanoparticle diameter $\delta = 20$ nm and incident wavelength $\lambda = 790$ nm; (b) $\delta = 100$ nm and $\lambda = 805$ nm; (c) $\delta = 200$ nm and $\lambda = 795$ nm; (d) $\delta = 200$ nm and $\lambda = 920$ nm.

Optics EXPRESS

Figure 7(a) shows the near-field amplitude distribution around the antenna and a 20 nm particle when the force is maximum at λ = 790 nm . The incident field amplitude was set to be 1 for all the near-field plots so that the field amplitude can also be read as amplitude enhancement factor. The field distribution is similar to that without the particle in Fig. 1(b). This implies that the field disturbance caused by the particle is not significant, which we already confirmed in the previous section through the comparison of the force between the two approaches. It is also clear from Fig. 6(a) that the inclusion of the particle to the system shows very little change in the resonance spectrum. The dipolar charges on the particle surface on the right side of Fig. 7(a) prove that the dipole approximation is valid for this size. In addition, the imaginary part of the complex charge dominates over the real part, which tells us that the system behaves simply like a driven oscillator.

The optical force then reaches its local maximum at the particle size of 100 nm, and the corresponding fields and polarization charges are shown in Fig. 7(b). They show that the larger particle has a stronger coupling with the antenna. Particularly, in the near-field plot, the field is intensely localized at the gap between the particle and the antenna. In the charge plot, on the other hand, the particle is still polarized like a dipole, but it has a higher charge density closer to the antenna. This is indicative of an attraction of opposite charges between the particle and the antenna, which can also be interpreted as optical binding [48,49]. The resonant wavelength of maximum force is also shifted from 790 nm to 805 nm as a result of the strong coupling.

As the particle size further increases, the optical force enters a new phase: its magnitude becomes much more extensive, and the force sign changes from negative (attracting the particle) to positive (pushing it away) depending on the incident wavelength of light. For example, the force magnitude exerted on a 200 nm particle is approximately 4 times larger than that on a 100 nm particle at each investigated points (the points B and C in Fig. 5).

The near-field and charge plots for the antenna with a 200 nm particle in Figs. 7(c) and 7(d) offer some insights into the underlying physics of these complex phenomena, and they have many interesting points to address. First of all, Fig. 7(c) shows that the particle couples with the antenna in a way that reinforces the antenna resonance; the factor of near-field amplitude enhancement reaches up to 50 (not obviously shown in the plot due to the uniform color bar scale), and the polarization charge magnitude is also larger compared to the other cases with the smaller particles. The charge plots on the right side of Fig. 7(c) also illustrate that the charges on the particle surface develop into a more complicated way, showing asymmetric multipole modes. The charges especially tend to concentrate on the side closer to the antenna and form the inverse mirror image on that face. This peculiar behavior of the charges may explain the extraordinary force that attracts the particle towards the antenna, which may also be understood as optical binding induced by the intense optical near-fields. Lastly, the real part of the charge now becomes comparable to its imaginary part. It implies that the particle and the antenna form a compound system, which is not anymore like a simple harmonic oscillator [47].

On the contrary, Fig. 7(d) shows the field and charge plots for the particle of the same size, 200 nm, but when the antenna is out of resonance, i.e., the incident wavelength is λ = 920 nm. At this wavelength, the antenna does not produce significant near-fields, which means that the gradient force would not be strong enough to trap the particle. At the same time, the scattering force acting in the direction of propagation scales up with the particle size since in first approximation it is proportional to the scattering cross-section. As a result, the net force, which is the sum of the gradient and scattering forces that are opposite each other, can push the particle away.

Figure 8 makes this argument more convincing. Figure 8(a) shows the dipole moment amplitudes for the antenna and the particle, computed from their surface polarization charges. The antenna's dipole moment has a maximum at λ = 800 nm where the antenna is on resonance. On the contrary, the particle's moment remains large for longer wavelengths. So at λ = 920 nm, which is the wavelength used in Fig. 7(d), the incident light mainly interacts with the particle, and therefore, the scattering force is likely to dominate the net force. In addition, if we compute

Optics EXPRESS

the scattering force acting on the 200 nm particle in the absence of the antenna under the same conditions, the force become 2.3 pN; this value is very close to the total force obtained from the computation with the antenna, which is 2.2 pN.

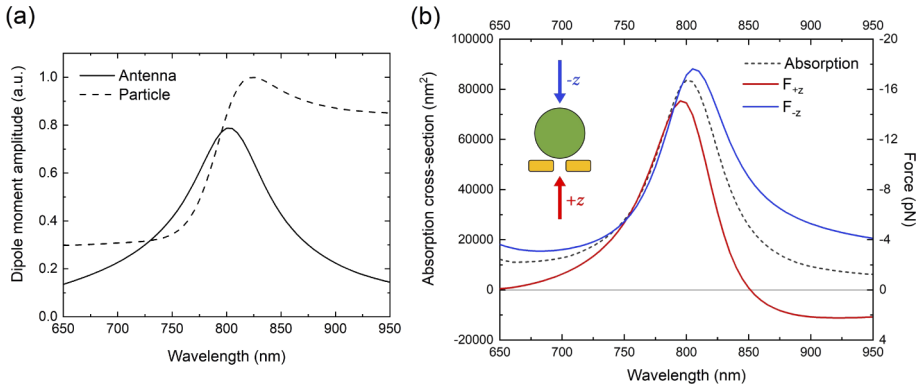

Fig. 8. Origin of the repulsive force. (a) Dipole moment amplitudes of the antenna (solid line) and the 200 nm particle (dashed line). (b) Force exerted on the 200 nm particle with two different illuminations: the light propagating $+z$ and $-z$ directions (red and blue solid lines). The absorption cross-section of the total system with the 200 nm particle (black dashed line).

On the other hand, Fig. 8(b) shows the force spectra on the 200-nm particle for two different illumination directions as well as the spectral response of the total system. The force spectra (the blue and red lines) are reversed in the vertical direction to make the comparison with the system response easier. So far, the light is incident in the $+z$ direction so that the scattering force is in the direction of pushing the particle away from the antenna. If the light is incident in the $-z$ direction such that the scattering force also pushes the particle toward the antenna as the gradient force does (the inset of Fig. 8(b)), we expect that the repulsive behavior will disappear. The blue line in Fig. 8(b) shows the force spectrum for this case and we do not see any repulsive force.

Another interesting point in Fig. 8(b) is that the force spectrum deviates from the spectrum of the absorption cross-section of the system (the black dashed line) in the opposite way depending on the direction of illumination. In this way, we can observe the contribution of the scattering force according to whether it is additive or subtractive to the gradient force.

3. Conclusion

We have compared the MST method with DA for force calculations to study how the interaction between a metallic particle and a trapping plasmonic dipole antenna influences the optical force. Quite surprisingly, and in spite of the strong coupling between both structures, the DA method still works very well, especially particles smaller than 15 nm. The discrepancy between the two approaches become noticeable for extreme cases, for example, when the antenna is on resonance, and the particle is in the location of high-intensity fields. In most cases, however, the DA method remains accurate and reliable. Besides that, we have studied the optical force in systems with larger particles, whose sizes are beyond the range of the dipole approximation. We have found different coupling regimes with large particles, where the particle polarization is much more complicated than a simple dipole. The force in such an intricate system has shown either attractive or repulsive behaviors depending on the excitation conditions, and the distribution of polarization charges on the structures at hand explain well these behaviors.

Optics EXPRESS

Funding

European Research Council (ERC-2015-AdG- 695206 Nanofactory).

Acknowledgments

We thank Prof. Q Han Park, Korea University, for helpful discussions.

Disclosures

The authors declare no conflicts of interest.

References

1. A. Ashkin, "Acceleration and trapping of particles by radiation pressure," Phys. Rev. Lett. **24**(4), 156–159 (1970).
2. A. Ashkin, J. M. Dziedzic, J. E. Bjorkholm, and S. Chu, "Observation of a single-beam gradient force optical trap for dielectric particles," Opt. Lett. **11**(5), 288–290 (1986).
3. A. Ashkin and J. M. Dziedzic, "Optical trapping and manipulation of viruses and bacteria," Science **235**(4795), 1517–1520 (1987).
4. S. M. Block, D. F. Blair, and H. C. Berg, "Compliance of bacterial flagella measured with optical tweezers," Nature **338**(6215), 514–518 (1989).
5. A. Ashkin, K. Schütze, J. M. Dziedzic, U. Euteneuer, and M. Schliwa, "Force generation of organelle transport measured in vivo by an infrared laser trap," Nature **348**(6299), 346–348 (1990).
6. M. D. Wang, H. Yin, R. Landick, J. Gelles, and S. M. Block, "Stretching DNA with optical tweezers," Biophys. J. **72**(3), 1335–1346 (1997).
7. D. G. Grier, "A revolution in optical manipulation," Nature **424**(6950), 810–816 (2003).
8. K. C. Neuman and S. M. Block, "Optical trapping," Rev. Sci. Instrum. **75**(9), 2787–2809 (2004).
9. M. Dienerowitz, M. Mazilu, and K. Dholakia, "Optical manipulation of nanoparticles: a review," J. Nanophotonics **2**(1), 021875 (2008).
10. C. Bradac, "Nanoscale optical trapping: A review," Adv. Opt. Mater. **6**(12), 1800005 (2018).
11. P. Zemánek, A. Jonáš, L. Šrámek, and M. Liška, "Optical trapping of nanoparticles and microparticles by a gaussian standing wave," Opt. Lett. **24**(21), 1448–1450 (1999).
12. L. Novotny, R. X. Bian, and X. S. Xie, "Theory of nanometric optical tweezers," Phys. Rev. Lett. **79**(4), 645–648 (1997).
13. A. N. Grigorenko, N. W. Roberts, M. R. Dickinson, and Y. Zhang, "Nanometric optical tweezers based on nanostructured substrates," Nat. Photonics **2**(6), 365–370 (2008).
14. M. Righini, A. S. Zelenina, C. Girard, and R. Quidant, "Parallel and selective trapping in a patterned plasmonic landscape," Nat. Phys. **3**(7), 477–480 (2007).
15. M. Righini, G. Volpe, C. Girard, D. Petrov, and R. Quidant, "Surface plasmon optical tweezers: Tunable optical manipulation in the femtonewton range," Phys. Rev. Lett. **100**(18), 186804 (2008).
16. M. Righini, P. Ghenuche, S. Cherukulappurath, V. Myroshnychenko, F. J. Garcia de Abajo, and R. Quidant, "Nano-optical trapping of rayleigh particles and escherichia coli bacteria with resonant optical antennas," Nano Lett. **9**(10), 3387–3391 (2009).
17. M. L. Juan, R. Gordon, Y. Pang, F. Eftekhari, and R. Quidant, "Self-induced back-action optical trapping of dielectric nanoparticles," Nat. Phys. **5**(12), 915–919 (2009).
18. M. L. Juan, M. Righini, and R. Quidant, "Plasmon nano-optical tweezers," Nat. Photonics **5**(6), 349–356 (2011).
19. R. Quidant, "Plasmonic tweezers–the strength of surface plasmons," MRS Bull. **37**(8), 739–744 (2012).
20. P. Padhy, M. A. Zaman, and L. Hesselink, "In-plane near-field optical barrier on a chip," Opt. Lett. **44**(8), 2061–2064 (2019).
21. V. Giannini, A. I. Fernández-Domínguez, S. C. Heck, and S. A. Maier, "Plasmonic nanoantennas: fundamentals and their use in controlling the radiative properties of nanoemitters," Chem. Rev. **111**(6), 3888–3912 (2011).
22. H. Fischer and O. J. F. Martin, "Engineering the optical response of plasmonic nanoantennas," Opt. Express **16**(12), 9144–9154 (2008).
23. R. D. Grober, R. J. Schoelkopf, and D. E. Prober, "Optical antenna: Towards a unity efficiency near-field optical probe," Appl. Phys. Lett. **70**(11), 1354–1356 (1997).
24. W. Zhang, L. Huang, C. Santschi, and O. J. F. Martin, "Trapping and sensing 10 nm metal nanoparticles using plasmonic dipole antennas," Nano Lett. **10**(3), 1006–1011 (2010).
25. K. B. Crozier, A. Sundaramurthy, G. S. Kino, and C. F. Quate, "Optical antennas: Resonators for local field enhancement," J. Appl. Phys. **94**(7), 4632–4642 (2003).
26. A. Ashkin, "Applications of laser radiation pressure," Science **210**(4474), 1081–1088 (1980).
27. P. C. Ke and M. Gu, "Characterization of trapping force on metallic mie particles," Appl. Opt. **38**(1), 160–167 (1999).
28. M. Pelton and G. W. Bryant, *Introduction to metal-nanoparticle plasmonics*, vol. 5 (John Wiley & Sons, 2013).

Optics EXPRESS

29. E. Prodan, C. Radloff, N. J. Halas, and P. Nordlander, "A hybridization model for the plasmon response of complex nanostructures," Science **302**(5644), 419–422 (2003).
30. J. R. Arias-Gonzalez and M. Nieto-Vesperinas, "Optical forces on small particles: attractive and repulsive nature and plasmon-resonance conditions," J. Opt. Soc. Am. A **20**(7), 1201–1209 (2003).
31. M. Pelton, M. Liu, H. Y. Kim, G. Smith, P. Guyot-Sionnest, and N. F. Scherer, "Optical trapping and alignment of single gold nanorods by using plasmon resonances," Opt. Lett. **31**(13), 2075–2077 (2006).
32. K. Svoboda and S. Block, "Optical trapping of metallic rayleigh particles," Opt. Lett. **19**(13), 930–932 (1994).
33. P. M. Hansen, V. K. Bhatia, N. Harrit, and L. Oddershede, "Expanding the optical trapping range of gold nanoparticles," Nano Lett. **5**(10), 1937–1942 (2005).
34. L. Bosanac, T. Aabo, P. M. Bendix, and L. B. Oddershede, "Efficient optical trapping and visualization of silver nanoparticles," Nano Lett. **8**(5), 1486–1491 (2008).
35. F. Hajizadeh and S. N. S.Reihani, "Optimized optical trapping of gold nanoparticles," Opt. Express **18**(2), 551–559 (2010).
36. C. F. Bohren and D. R. Huffman, *Absorption and Scattering of Light by Small Particles* (Wiley Interscience, 1983).
37. P. B. Johnson and R. W. Christy, "Optical constants of the noble metals," Phys. Rev. B **6**(12), 4370–4379 (1972).
38. P. Gay-Balmaz and O. J. F. Martin, "Electromagnetic scattering of high-permittivity particles on a substrate," Appl. Opt. **40**(25), 4562–4569 (2001).
39. K. C. Vernon, A. M. Funston, C. Novo, D. E. Gómez, P. Mulvaney, and T. J. Davis, "Influence of particle–substrate interaction on localized plasmon resonances," Nano Lett. **10**(6), 2080–2086 (2010). PMID: 20476750.
40. A. M. Kern and O. J. F. Martin, "Surface integral formulation for 3d simulations of plasmonic and high permittivity nanostructures," J. Opt. Soc. Am. A **26**(4), 732–740 (2009).
41. A. Ji, T. V. Raziman, J. Butet, R. P. Sharma, and O. J. F. Martin, "Optical forces and torques on realistic plasmonic nanostructures: a surface integral approach," Opt. Lett. **39**(16), 4699–4702 (2014).
42. J. Kim and O. J. Martin, "Data set for the manuscript: The different coupling regimes for a plasmonic particle in a plasmonic trap," https://doi.org/10.5281/zenodo.3525240 (2019).
43. P. C. Chaumet and M. Nieto-Vesperinas, "Time-averaged total force on a dipolar sphere in an electromagnetic field," Opt. Lett. **25**(15), 1065–1067 (2000).
44. L. Novotny and B. Hecht, *Principles of Nano-Optics* (Cambridge University, Cambridge, 2012), 2nd ed.
45. L. Neumeier, R. Quidant, and D. E. Chang, "Self-induced back-action optical trapping in nanophotonic systems," New J. Phys. **17**(12), 123008 (2015).
46. L. Huang and O. J. F. Martin, "Reversal of the optical force in a plasmonic trap," Opt. Lett. **33**(24), 3001–3003 (2008).
47. T. V. Raziman and O. J. F. Martin, "Does the real part contain all the physical information?" J. Opt. **18**(9), 095002 (2016).
48. M. M. Burns, J.-M. Fournier, and J. A. Golovchenko, "Optical binding," Phys. Rev. Lett. **63**(12), 1233–1236 (1989).
49. F. Dapasse and J. M. Vigoureux, "Optical binding force between two rayleigh particles," J. Phys. D: Appl. Phys. **27**(5), 914–919 (1994).